JGR Atmospheres

RESEARCH ARTICLE
10.1029/2019JD030689

# Decelerated Greenland Ice Sheet Melt Driven by Positive Summer North Atlantic Oscillation

**Ruomei Ruan[1,2], Xianyao Chen[1,2,3], Jinping Zhao[1,2], William Perrie[4], Ruth Mottram[5], Minghong Zhang[4], Yina Diao[6], Ling Du[6], and Lixin Wu[1,2]**

[1]Key Laboratory of Physical Oceanography, Ocean University of China, Qingdao, China, [2]Qingdao National Laboratory of Marine Science and Technology, Qingdao, China, [3]Key Laboratory of Numerical Modelling for Atmospheric Sciences and Geophysical Fluid Dynamics, Beijing, China, [4]Fisheries and Oceans Canada, Bedford Institute of Oceanography, Dartmouth, Nova Scotia, Canada, [5]Danish Meteorological Institute, Copenhagen, Denmark, [6]College of Oceanic and Atmospheric Sciences, Ocean University of China, Qingdao, China

**Key Points:**
- Greenland Ice Sheet exhibits decelerated melt since 2013
- The deceleration is due to increased cloud during positive summer NAO
- The accelerated and decelerated GrIS melt will reoccur on decadal time scale

**Correspondence to:**
X. Chen,
chenxy@ouc.edu.cn

**Citation:**
Ruan, R., Chen, X., Zhao, J., Perrie, W., Mottram, R., Zhang, M., et al. (2019). Decelerated Greenland Ice Sheet melt driven by positive summer North Atlantic Oscillation. *Journal of Geophysical Research: Atmospheres*, *124*, 7633–7646. https://doi.org/10.1029/2019JD030689

Received 26 MAR 2019
Accepted 30 JUN 2019
Accepted article online 12 JUL 2019
Published online 27 JUL 2019

**Abstract** The abrupt deceleration of accelerated Greenland Ice Sheet (GrIS) melting since 2013, after a period of acceleration previously noted, is studied here. It is shown that the deceleration of GrIS melting since 2013 is due to the reduction in short-wave solar radiation in the presence of increasing total cloud cover, which is driven by a more persistent positive summer North Atlantic Oscillation on the decadal time scale. By presenting the coherence with the temperature variability at the weather stations in Greenland, which have century-long records, we deduce that the acceleration of GrIS melting during the early 2000s and the subsequent deceleration since 2013 will reoccur frequently on decadal time scales, with the amplitude nearly half of the multidecadal warming trend of the GrIS melt. It can reduce the mass loss from the GrIS on short to medium time scales but is unlikely to halt mass loss related to climate change in the future. This finding highlights the importance of internal climate variability on the mass budget of the GrIS and therefore on predictions of future global sea level change and may help to assist planning for associated social and economic consequences.

**Plain Language Summary** The Greenland Ice Sheet (GrIS) mass change and its contribution to the global sea level variability is a topic that naturally piques our curiosity. Since the satellite first captured the Greenland-wide ice sheet mass variability in 2002, the GrIS experienced accelerated melting, leading to global sea level acceleration. The long-term GrIS melting depends on climate change such as greenhouse warming. However, recently, this acceleration is slowed down due to the summer North Atlantic Oscillation phase changing to positive. We use century-long surface temperature records as index to estimate the contribution of this slowdown phenomenon and find that the amplitude of this internal variability is nearly half of the multidecadal warming trend of the GrIS; therefore, this cycle can slow down but cannot stop the loss of the Greenland Ice Sheet mass at present and in the near future. This finding highlights the role of the internal variability of the GrIS on predictions of future global sea level change and the associated social and economic consequences.

## 1. Introduction

The Greenland Ice Sheet (GrIS) acts as a cog in the global climate machine. Meltwater from the ice sheet will not only raise the global sea level but also contribute to freshening in the subpolar North Atlantic Ocean, potentially weakening deep convection and reducing the Atlantic Meridional Overturning circulation. This may lead to further feedback effects on the global thermohaline circulation and hence the global heat distributions (Chen & Tung, 2018; Hu et al., 2011).

The GrIS mass balance in a warming climate is between increased precipitation in the form of snow on Greenland caused by increased ocean evaporation and enhanced melting of the ice sheet surface combined with increased coastal glacier discharge (Velicogna & Wahr, 2006). Model predictions agree with observations that SMB (surface mass balance) rather than ice discharge ($D$) will dominate the GrIS contribution to sea level rise in the 21st century (Enderlin et al., 2014). Nevertheless, surface melting interrelates with $D$, and the ice flow increases when melting enhances in summer (Zwally et al., 2002). However, the relative contribution of SMB and $D$ to GrIS mass balance is not constant. The accelerated outflow of glaciers is the result of the interaction of atmosphere and ocean (Straneo et al., 2010).

Hanna et al. (2010) attributed the thinning GrIS, increasing runoff, and significant rising summer temperature since the 1990s to global warming. The surface melting process in Greenland accounts for about half of the total mass loss of GrIS (van den Broeke et al., 2009). And this proportion is even greater in the case of long-term increase of surface temperature (Smith et al., 2014). Surface energy balance (SEB) plays an important role in GrIS mass balance, which includes radiation and turbulence heat flux, and regulates surface melt by controlling surface temperature (Miller et al., 2017). Clouds (especially low-level liquid clouds) have an important effect on the net surface radiation flux (Walsh & Chapman, 1998), thereby affecting the SEB. Studies have also shown that GrIS is vulnerable to climate warming caused by human behavior (Gregory et al., 2004; Velicogna & Wahr, 2006). However, due to the short data span of the overall GrIS mass observation, there is no persuasive argument about long-term variation of GrIS.

## 2. Data and Methods

### 2.1. Variation Characteristics of GrIS Mass

Observations of the mass of the GrIS from the Gravity Recovery and Climate Experiment (GRACE) satellite (Chen, 2006) are used to study the mass balance of GrIS. The GRACE satellite mission, which was in operation from March 2002 to June 2017, consists of two identical spacecrafts flying in the same orbit, about 220 km apart at a height of approximately 500 km, orbitting the Earth in about 95 min. The GRACE data we use are the GFZ RL05 level-3 data with a horizontal resolution of 1 degree.

The time series of the data with 13 missing months is from January 2003 to December 2016. The missing month is filled by linear interpolation. The original GRACE data are liquid water equivalent thickness with the unit of centimeter. In order to get the mass changing of GrIS, we convert it into gigatons by multiplying grid area and density of the ice.

The cumulative melt area of the GrIS is based on the daily area experiencing melt for the annual melt season (April through October) in millions of square kilometers over 39 years (1979 to 2017) from the National Snow and Ice Data Center. Daily surface melt data are provided by Thomas Mote at University of Georgia since 1979.

The annual total mass of the GrIS is determined by the net annual increase and decrease of the mass. The net annual increase is computed as the maximum mass in March-April (the period when the net heat flux is negative) in the next year minus the minimum mass in September-October (the period when the net heat flux is positive) in this year. The net annual decrease is computed as the minimum mass in September-October minus the maximum mass in March-April in the same year.

To investigate GrIS mass balance, we use European Centre for Medium-Range Weather Forecasts Re-Analysis (ERA)-Interim monthly means of daily forecast accumulations surface total precipitation and snowfall data since 1979 (Dee et al., 2011).

### 2.2. Comparing the Mass Budget With SEB

We compute the equivalent mass change due to positive (negative) net heat flux which is dominated by the net shortwave (longwave) radiation by integrating it during the period when the net heat flux is positive (negative). The surface heat flux data are obtained from the National Centers for Environmental Prediction (NCEP)/National Center for Atmospheric Research (NCAR) Reanalysis 1 data (Kalnay et al., 1996), which are provided by the National Oceanic and Atmospheric Administration/Oceanic and Atmospheric Research/Earth System Research Laboratory's Physical Sciences Division, Boulder, Colorado, USA. The net heat flux is given by the sum of net shortwave radiation (SWnet), net longwave radiation (LWnet), sensible heat flux (SHF), latent heat flux (LHF), and the ground flux (negligible). All of the surface heat fluxes are defined as positive when they add heat to the surface. The SWnet is given by $\mathrm{SWnet} = \mathrm{SWD} * (1 - \alpha)$, where SWD is downward shortwave radiation and $\alpha$ albedo over Greenland surface. The LWnet is calculated as the difference between downward longwave radiation (LWD) and upward longwave radiation (LWU). The daily SWnet, LWnet, SHF, and LHF obtained from NCEP are used to compute the net heat flux.

Net heat flux is controlled by the total cloud cover. We compute the linear trend of the total cloud cover at each grid box of Greenland. Figures 3c and 3d are based on CERES satellite data (Allan, 2011), while Figures 4b, 4c, 4e, and 4f are based on NCEP/NCAR Reanalysis 1 data.

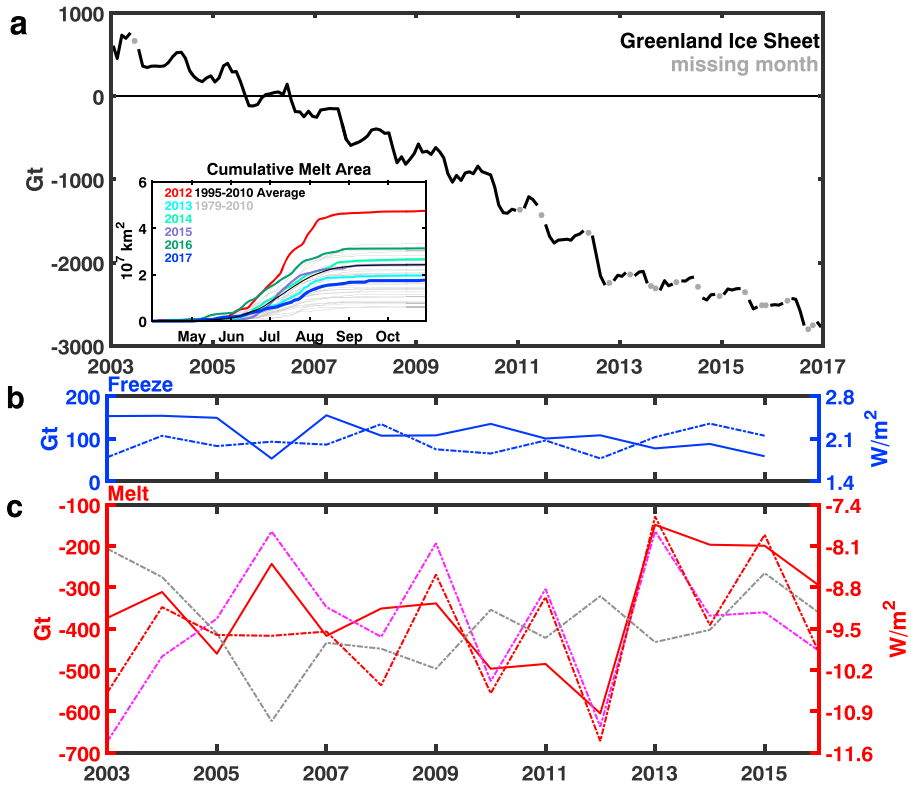


**Figure 1.** Greenland Ice Sheet (GrIS) mass change. (a) The mass of GrIS from GRACE satellite since 2003. Gray dots denote the missing month which is filled by linear interpolation. The inset shows the cumulative melt area since 1979 from the National Snow and Ice Data Center daily surface melt data. The light gray lines are for 1979–2010. The black line shows the average area during 1995–2010. The color lines are those from 2012 to 2017. (b) Net annual increase (solid blue lines) and (c) decrease (solid red lines) of GrIS mass derived from GRACE satellite observations. The dashed line in blue/red is the integral net heat flux calculated with National Centers for Environmental Prediction/National Center for Atmospheric Research Reanalysis 1 data during the freeze/melt time. The net heat flux components (magenta line = shortwave; gray line = the summation of longwave, sensible, and latent) variation during melt season. GrIS = Greenland Ice Sheet.

The sea surface temperature (SST) data used in this paper are the daily optimum interpolation High Resolution Blended Analysis SST (Banzon et al., 2016) during 1982–2016 supported by National Oceanic and Atmospheric Administration/OAR/Earth System Research Laboratory PSD, Boulder, Colorado, USA.

### 2.3. Ensemble Empirical Mode Decomposition Method

The method used to decompose the GrIS and the Greenland temperature (GrT) time series is the Ensemble Empirical Mode Decomposition (EEMD; Wu & Huang, 2009), which was developed on the basis of the empirical mode decomposition (EMD) method (Huang et al., 1998). The EMD and EEMD methods have been widely applied to oceanic and climatic time series analysis. Here we briefly introduce the general decomposition procedure and mainly introduce how to combine the adjacent intrinsic mode functions (IMFs) to get physical modes.

#### 2.3.1. Decomposition

In EMD, a time series $x(t)$ is decomposed into a set of amplitude-frequency modulated oscillatory functions (so-called IMFs) $C_j(t), j = 1, 2,.. n$ and a residual $R(t)$, which has at most one extremum: $x(t) = \sum_{j=1}^{n} C_j(t) + R(t)$ through a sifting process, the following is undertaken: (1) locate all maxima and minima and connect all maxima (minima) with a cubic spline as an upper (lower) envelope of the time series; (2) compute the difference between the time series and the mean of the upper and lower envelopes to yield a new time series $h(t)$; (3) for the time series $h(t)$, repeat steps 1 and 2 until upper and lower envelopes are symmetric with respect to zero mean under the stopping criteria, then an IMF, $C_j(t)$, is derived as the time series $h(t)$; and

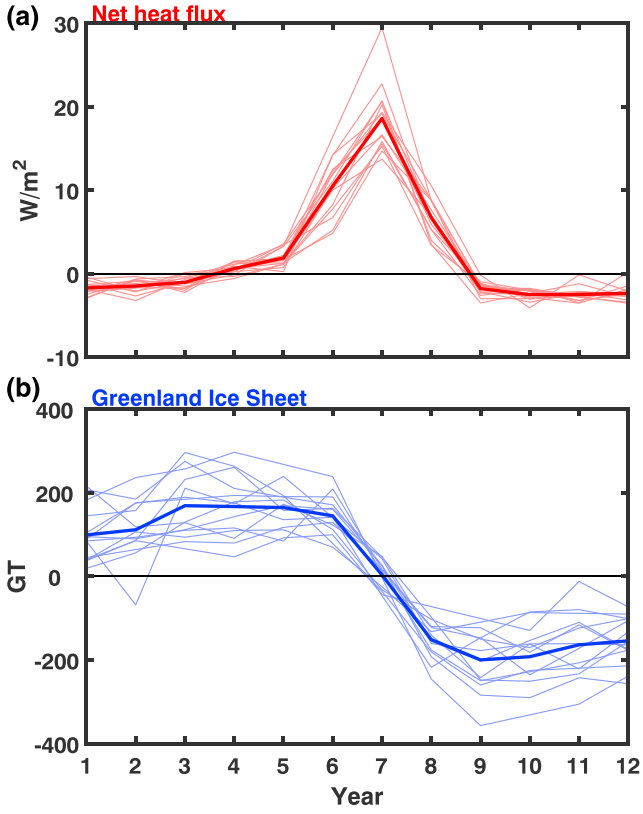


**Figure 2.** Seasonal variation of surface net heat flux and the GrIS mass. (a) Monthly surface net heat flux over Greenland during 2003–2016 (thin solid lines) and their monthly mean (thick line). (b) Same as (a) but for the monthly GrIS mass. GrIS = Greenland Ice Sheet.

(4) subtract $C_j(t)$ from original time series to yield a residual $R(t)$ and treat $R(t)$ as the original time series and repeat steps 1–3 until the residual $R(t)$ becomes a monotonic function or a function with only one extremum; then, the whole sifting process is completed and all IMFs and the residual function, namely, the intrinsic trend of $x(t)$, are obtained.

The EEMD approach is based on EMD. In EEMD, multiple noise realizations are added to the time series $x(t)$, from which an ensemble average of the corresponding IMFs are extracted to yield scale-consistent signals. The main steps in the EEMD are as follows: (1) add a white noise series to the targeted data; (2) decompose the data with the added white noise into IMFs; (3) repeat steps 1 and 2 again and again, but with different white noise series each time; and (4) obtain (ensemble) means of the respective IMFs of the decompositions as the final result. The advantage of the EEMD is that by using an ensemble mean, nonphysical oscillations due to random data errors are reduced and thus low-frequency modes are more accurate.

It is proved that the added white noise with the variance $\sigma$ will have at most $\sigma/\sqrt{N}$ impact on the resulted IMFs, where $N$ is the number of ensemble members. When $N$ increases, this impact is negligibly small. In this paper, we always use the white noise with variance relative to the variance of the original time series, and $N = 1000$ ensemble members.

#### 2.3.2. Combination

IMFs derived by EMD or EEMD methods are almost orthogonal with each other in the context of Reynold's mean. This means that the overall mean of one IMF is nearly zero on the longer time scales represented by the other IMFs, and any two IMFs with different time scales can be linearly combined in the time domain to yield another time series, which is still orthogonal with other IMFs. This important feature is helpful for identifying common variability between the two time series with different length.

In this paper, the follow procedure is applied:

First, we decompose the GrIS summer melt into its IMFs and remove the IMF with the highest interannual variability, which did not exhibit increasing trend during 2003–2012 and the decreasing trend since 2013. Then, we keep the remaining lower frequency components as the GrIS summer melt during 2003–2016.

Second, we decompose the summer GrT into its IMFs and compute the mean period of each IMF. The first IMF of the summer GrT is of interannual variability, which did not exhibit increasing trend during 2003–2012 and the decreasing trend since 2013, either.

Third, we combine IMFs 2, 3, 4, and 5 of the summer GrT, choose the subsection of the resulting time series in the period of 2003–2016, and compute the correlation coefficient with the GrIS summer melt. When we get the maximum correlation coefficient, we obtain the combination of the corresponding IMFs of the summer GrT as the same variability of the GrIS summer melt; the other IMFs remain unchanged (Figure 9).

Following the procedures above, we can identify that the accelerated melt during 2003–2012 and the decelerated melt during 2013–2016 of the GrIS share similar variability with the summer GrT on the decadal and interdecadal time scales.

The data sets that we used to calculate GrT from Danish Meteorological Institute (DMI) are introduced in DMI Report No. 18-08 (John Cappelen; Weather observations from Greenland 1958–2017) and DMI Report No. 18-04 (John Cappelen (ed.); Greenland-DMI Historical Climate Data Collection 1784–2017). The weather stations in Greenland provide continuous temperature observations. We use 72 weather stations in Greenland, of which 68 started their temperature observations from 1958 and four have century-long continuous records. The positions of the stations are shown in Figure 7.

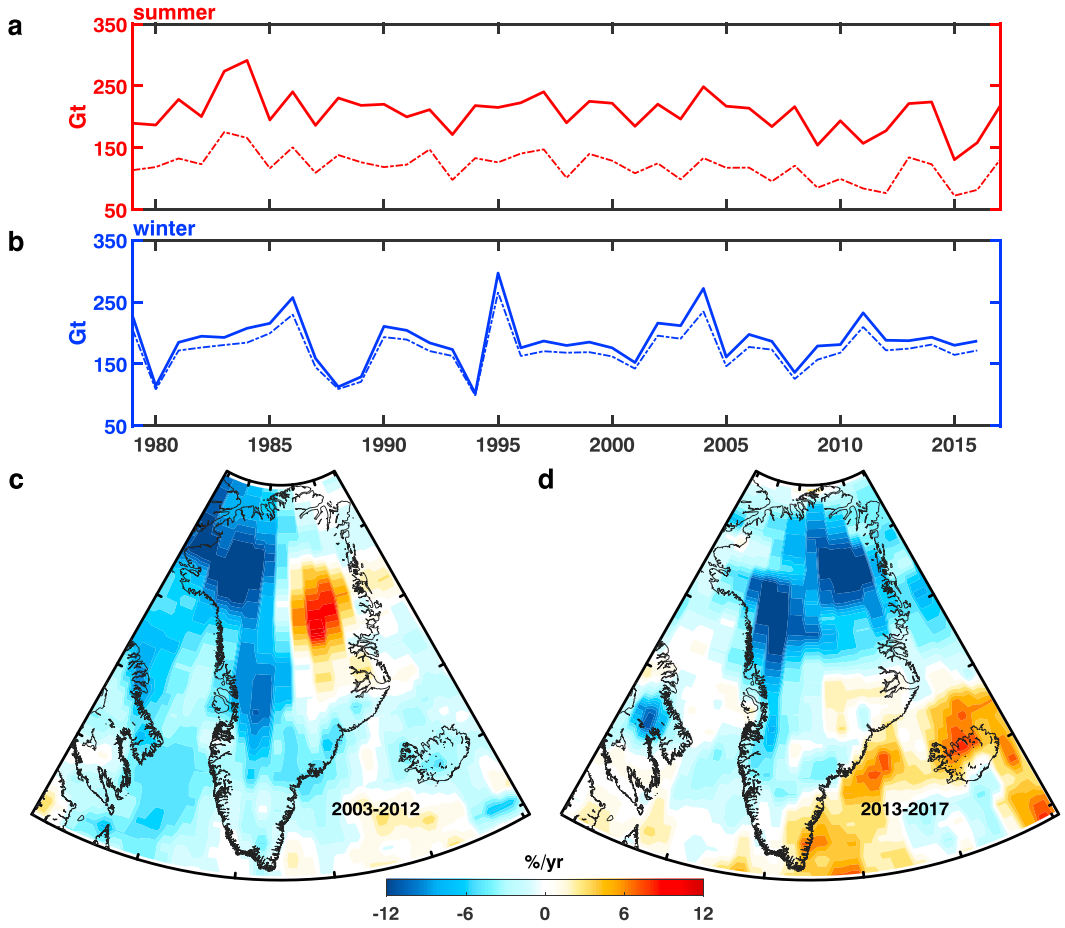


**Figure 3.** Greenland Ice Sheet mass budget and surface energy balance. The precipitation (solid line) and snowfall (dashed line) annual time series (a) in summer and (b) in winter. The linear trend of the total cloud cover during (c) 2003–2012 and (d) 2013–2016.

### 2.4. The Dynamics of Total Cloud Cover Change Over Greenland in a North Atlantic Perspective

We use monthly mean of sea level pressure (SLP) and geopotential height of the 500 hPa pressure level from the European Centre for Medium-Range Weather Forecasts ERA-20C reanalysis (Belleflamme et al., 2015) to calculate their regression patterns upon the net annual GrIS melt during 2003–2016 and the combined IMFs 2–4 of the Greenland temperature during 1910–2010.

Monthly mean SLP data from ERA-Interim and ERA-20C reanalysis data sets is used to calculate the summer North Atlantic Oscillation (sNAO) index, which is defined as the first eigenvector of pressure at mean sea level anomalies over the extratropical European-North Atlantic sector (25–70°N, 70°W to 50°E) in summer (June-July-August) during 2003–2016 and 1910–2010, respectively. According to EEMD method, the combined IMFs 3–6 of sNAO index has the maximum correlation with the combined IMFs 2–4 of the Greenland summer temperature. We also present the spatial patterns by projecting the mean summer SLP and Z500 during 2003–2016 and 1910–2010 onto the combined IMFs 3–6 of SNAO time series, respectively.

## 3. Results

### 3.1. Slowing Down of GrIS Melt Rates

Satellite observations from altimetry and GRACE show the accelerated GrIS melting since 1990s led to an accelerated rise in global mean sea level (GMSL) from 2.4 ± 0.2 mm/year in 1993 to 2.9 ± 0.3 mm/year in 2014 (Chen et al., 2017), and the contribution from Greenland is 0.76 ± 0.1 mm/year for the period 2005 to present (Cazenave, 2018).

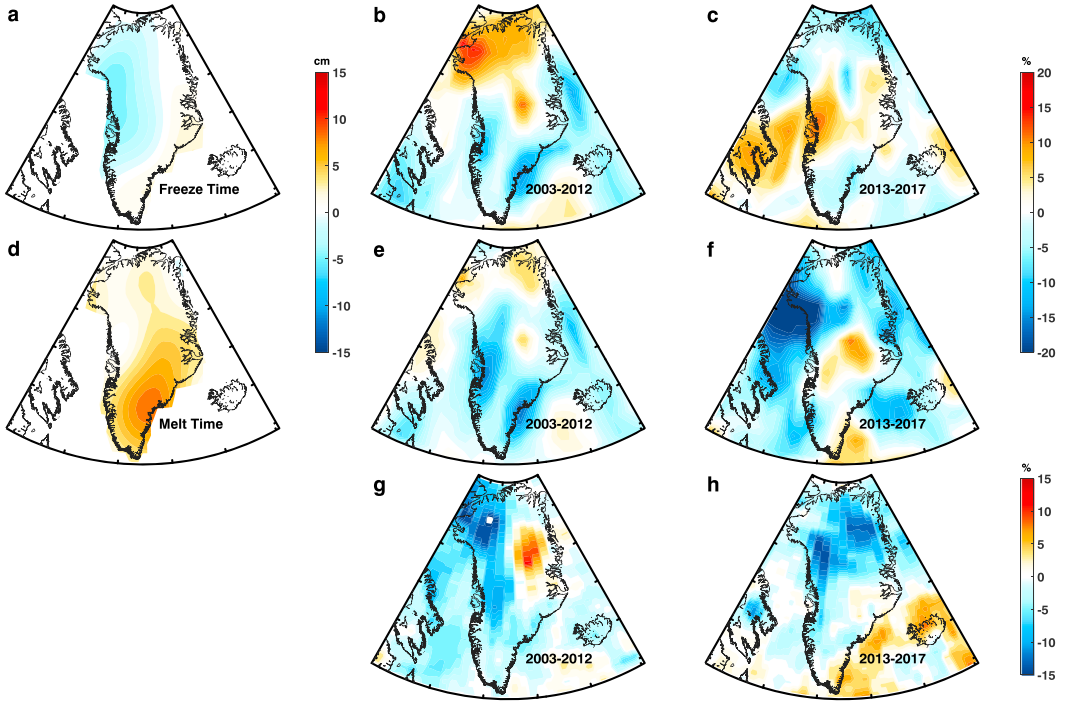


**Figure 4.** Spatial patterns of GrIS mass change and total cloud cover. The spatial pattern of (a) the net increase and (d) the net loss of the GrIS mass during 2003–2016. The linear trend of total cloud cover over Greenland in the winter of (b) 2003–2012, and (c) 2013–2017, based on National Centers for Environmental Prediction/National Center for Atmospheric Research Reanalysis 1 data set. (e, f) Same as (b) and (c), respectively, but for the summer. (g, h). Same as (e) and (f), respectively, but based on the satellite CERES data set. GrIS = Greenland Ice Sheet

However, recent GRACE and GPS observations showed the abrupt deceleration of the GrIS melt since 2013 (Figure 1a). The GrIS lost mass at a rate of about 102 Gt/year in early 2003, increased to 393 Gt/year during 2012–2013, but suddenly reduced to no more than 75 Gt/year during 2013–2014 (Bevis et al., 2019). It is suggested that this deceleration is due to the increased snowfall accumulation driven by the positive phase of sNAO (Chen et al., 2015; Folland et al., 2009).

The time scale of this deceleration is of importance on reducing the uncertainty of future projection of the GrIS variability and global sea level change. It is suggested that the deceleration during 2013–2014 has ended because the sNAO turned to negative in 2015 again (Bevis et al., 2019). However, Figure 1a shows that, except for the unusual summer melting in 2012 (Hanna et al., 2008), the total melt area calculated with daily surface melt data in Greenland from National Snow and Ice Data Center in the other years in the 2010s are all less than those exhibited during the melt seasons of the previous decade. Among these, the lowest is 2017. In order to understand the impacts and the time scales of this deceleration, we here further investigate the GrIS variability during the GRACE era, by comparing the temperature records in Greenland with century-long records.

### 3.2. Mechanisms Governing the GrIS Mass Balance

To appreciate the time scale of this deceleration since 2013, we first investigate the mechanism governing the loss and recover of the GrIS mass during the GRACE era in a North Atlantic perspective.

The GrIS mass variability is controlled by the balance between accumulation (including snowfall, precipitation, and basal freezing) and losses (including evaporation, surface melt and run off, and ice discharge) over the whole island. Figures 1b and 1c compare the net annual increase and decrease of the GrIS mass during the GRACE era. During the freezing season (the period with negative net heat flux over Greenland, Figure 2 ), the net annual increase of the GrIS mass, computed as the maximum mass in the following March-April minus the minimum mass in September-October, slightly decreased from about 120 Gt in 2003–2004 to 60 Gt in 2015. During the melting season (the period with positive net heat flux over Greenland, Figure 2), the net

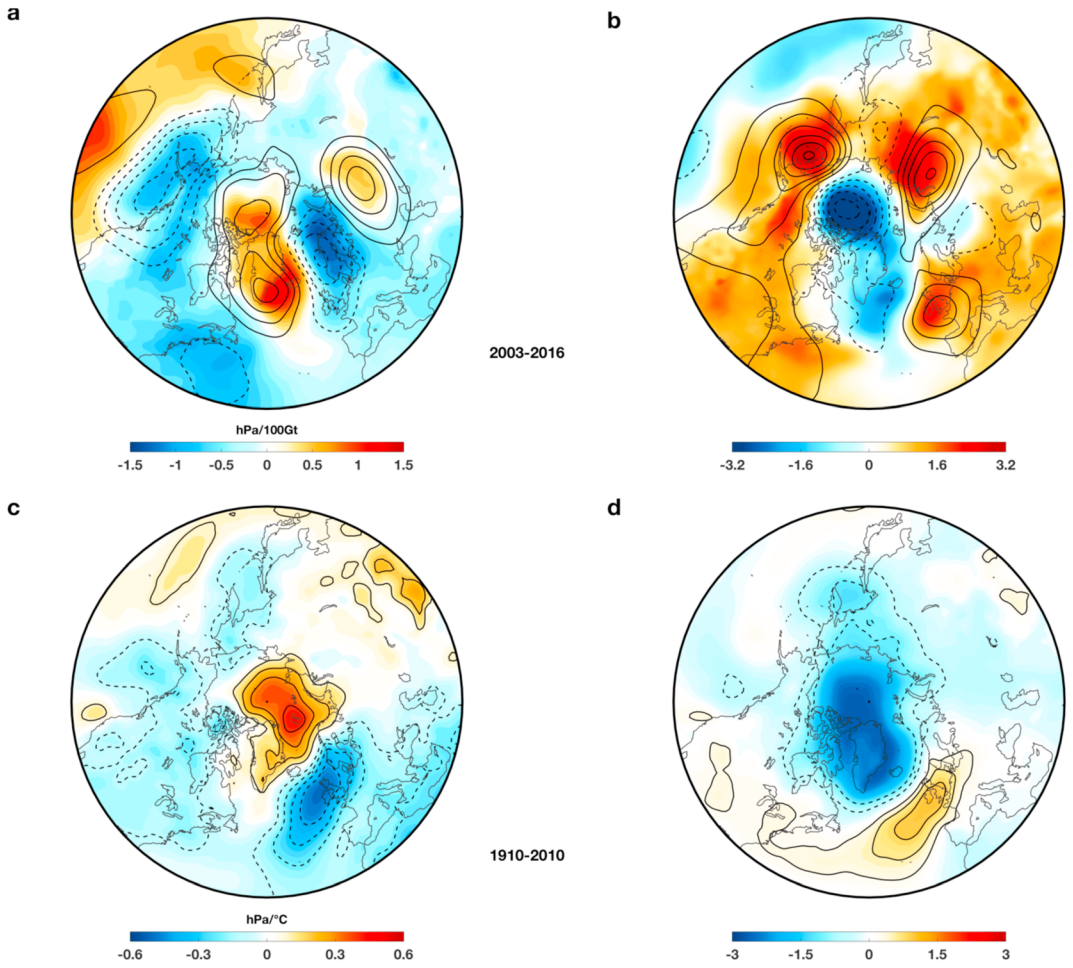


**Figure 5.** Atmospheric configurations over Greenland. (a, b) Spatial patterns by projecting the sea level pressure (color shading) and Z500 (contour line) upon (a) the Greenland Ice Sheet and (b) the IMFs 3–6 of the sNAO index during 2003–2016, respectively. (c, d) Same as (a) but for (c) the IMFs 2–4 of the GrT and (d) the IMFs 3–6 of the sNAO index during 1920–2010. The positive (negative) value is in solid (dashed) line. The contour interval is 50 m. IMFs = intrinsic mode functions; sNAO = summer North Atlantic Oscillation; GrT = Greenland temperature.

annual decrease of the GrIS mass, computed as the minimum mass in September-October minus the maximum mass in March-April of same the year, accelerated from about 350 Gt in 2003 to more than 600 Gt in 2012. After an extreme year of the GrIS mass loss in 2012 (Nghiem et al., 2012**;** Tedesco et al., 2013) the rate of mass loss dramatically decreased since 2013 and has returned to about the same level (or even less) as was observed during 2004–2005. This indicates that the deceleration in GrIS mass loss since 2013 is mostly attributable to a reduction in the total mass loss during the summer season.

It is suggested that the abrupt deceleration during 2013–2014 is due to the increasing accumulated snowfall as an impact of increased synoptic cyclonic activities during positive sNAO (Bevis et al., 2019; Chen et al., 2015). But the atmospheric reanalysis data set ERA-Interim shows that the overall precipitation, evaporation, and the snowfall in summer season over Greenland exhibited neither increasing nor decreasing trends during the last decade (Figure 3a), and in winter season, there is slightly decreasing trend, which is opposite to the increase of the GrIS mass since 2013. Therefore, the deceleration in GrIS mass loss is very likely dominated by reductions in surface melting and ice discharge, which is also correlated with the surface melting (Enderlin et al., 2014).

Based on the budget of the SMB, we compare the equivalent ice loss due to the surface heat fluxes, including shortwave radiation, longwave radiation, SHF, and LHF. As shown in Figure 1b, the GrIS mass change is highly correlated with the integrated positive net heat flux variability ($r$ = 0.68), and the deceleration in

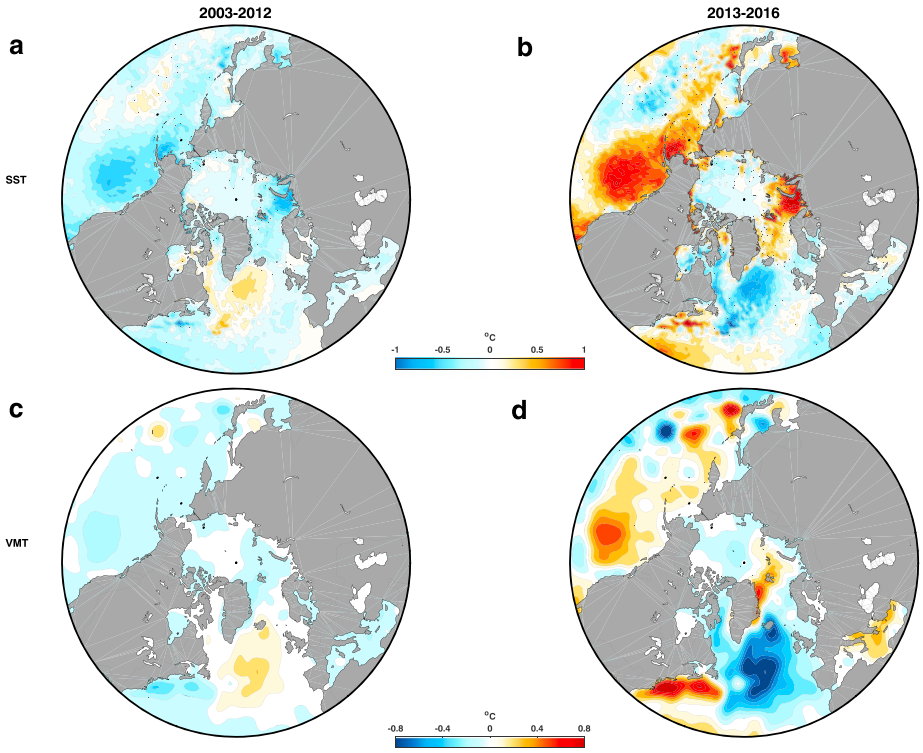


**Figure 6.** Mean SST and VMT of North Atlantic. The summer (June-July-August) mean SST in the North Atlantic subpolar gyre during (a) 2003–2012 and (b) 2013–2016. (c, d). Same as (a) and (b) but for the VMT. SST = sea surface temperature; VMT = volume mean temperature.

GrIS melt is dominated by the reduction in incoming shortwave radiation (dashed line in Figure 1b), computed as the integrated incoming shortwave radiation at the period with positive net heat flux during the summer season. The incoming shortwave radiation is determined by changes of the total cloud cover and the surface albedo. Figure 3c shows that the total cloud cover decreased with a rate of around 0.5% per year before 2013 in most of Greenland except the northeast area. As a result, the melt-albedo feedback is enhanced (Hofer et al., 2017) and the increased shortwave radiation over the low albedo ablation zone leads to accelerated melt of the GrIS (Box et al., 2012; Franco et al., 2013; van Angelen et al., 2012). Since 2013, the total cloud cover over most of southeast Greenland increased at a rate of more than 0.1% per year (Figure 3d). Although over northwest Greenland, the total cloud cover continued to decrease at an even higher rate than the previous decade, the overall pattern is that it increased over the entire island and its spatial structure also tended to correlate very well with the pattern of the GrIS melt in subsequent years. With these results, we emphasize the role of the increased total cloud cover during the summer season on the change in the volume of the GrIS. It is also consistent with the finding that the increased cloud in the winter can prevent the loss of outgoing longwave radiation and thereby reduces the refreezing of meltwater, enhancing the meltwater runoff and the GrIS mass loss (van Tricht et al., 2016). This impact is exhibited in the slightly decreased trend of freezing and integral net heat flux during winter seasons (Figures 3a and 4), though it is about 2 times smaller than the melting of the GrIS during summer seasons, that is, the impacts of the SWnet.

Figure 5a presents the spatial patterns by projecting the mean summer SLP and geopotential height of the 500-hPa pressure level (Z500) during 2003–2016 onto the summer GrIS melting time series. The negative correlation (high SLP corresponding to less GrIS mass or more melt) over Greenland and extending to most of the Arctic resembles the spatial pattern of the positive phase of sNAO (Folland et al., 2009).

During the sNAO− over the period 2003–2012, the weakening of the high SLP over northwest Europe and the Icelandic Low (positive SLP anomaly over Greenland) suggest reduction in cyclone activity and the

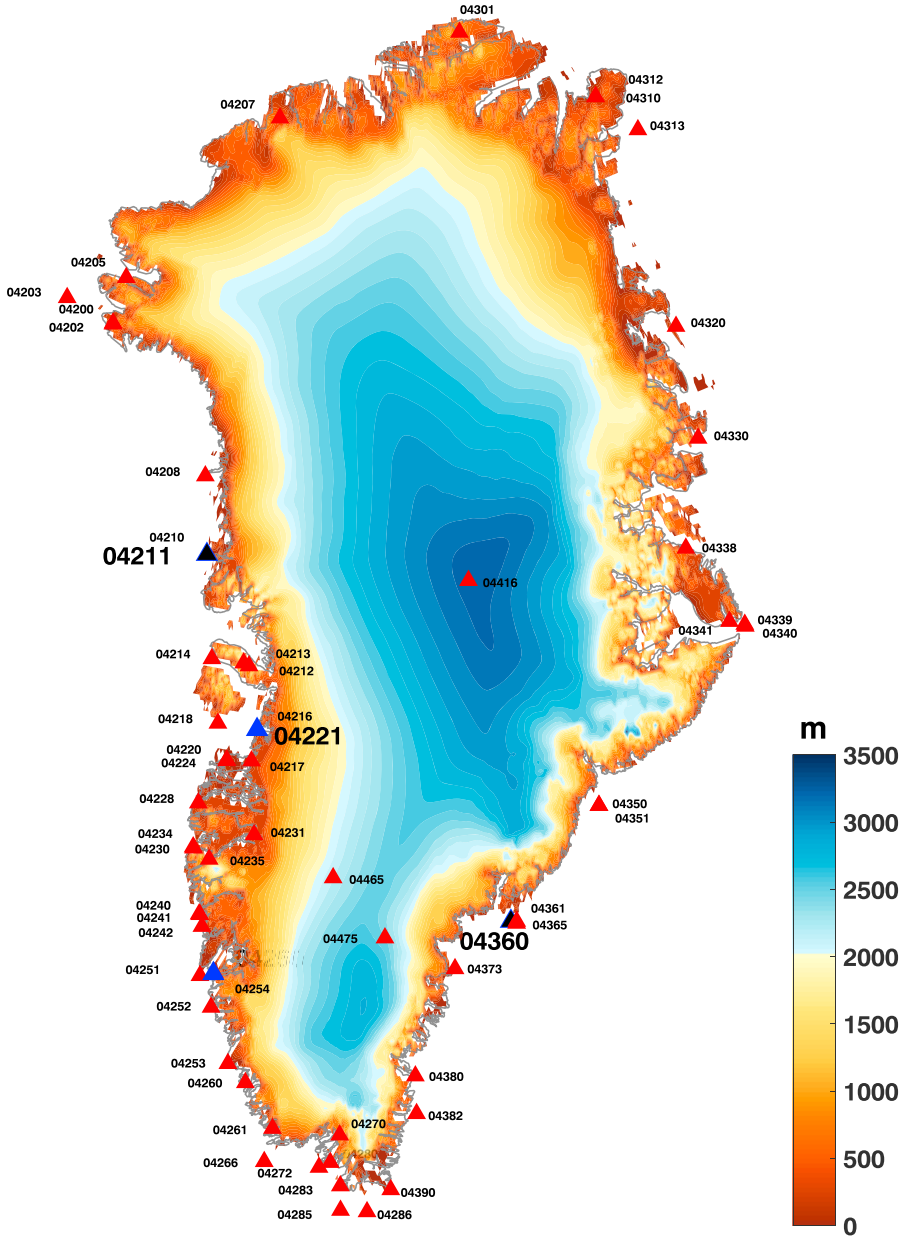


**Figure 7.** Weather Stations in Greenland. Sixty-eight weather stations with temperature observations since 1958 (red triangle) and four stations with century-long continuous records (blue triangles). Terrain's height is shown in shading color.

total cloud cover over the subpolar North Atlantic region (Figure 3c), thereby accelerating surface melting, as found in previous studies (Fettweis et al., 2011; Fettweis et al., 2013).

During sNAO+, a strengthened Icelandic Low and an intensified Azores high extends to northwest Europe (Figures 5a and 5b). This feature corresponds to a poleward shift of storm tracks over the North Atlantic due to intensified westerlies, resulting from deepening of the northern American trough (contours in Figure 5a). This kind of atmospheric configuration provides a rising condition for the air mass, both resulting in increased cloud cover and decreased incoming shortwave radiation.

The lower SLP over Greenland is also consistent with the dramatic cooling of the northern North Atlantic Ocean during the same period. On the surface, the mean summer SST in the North Atlantic subpolar gyre is more than 2 °C colder than the SST during 2003–2013; in the upper 300 m, the volume mean ocean

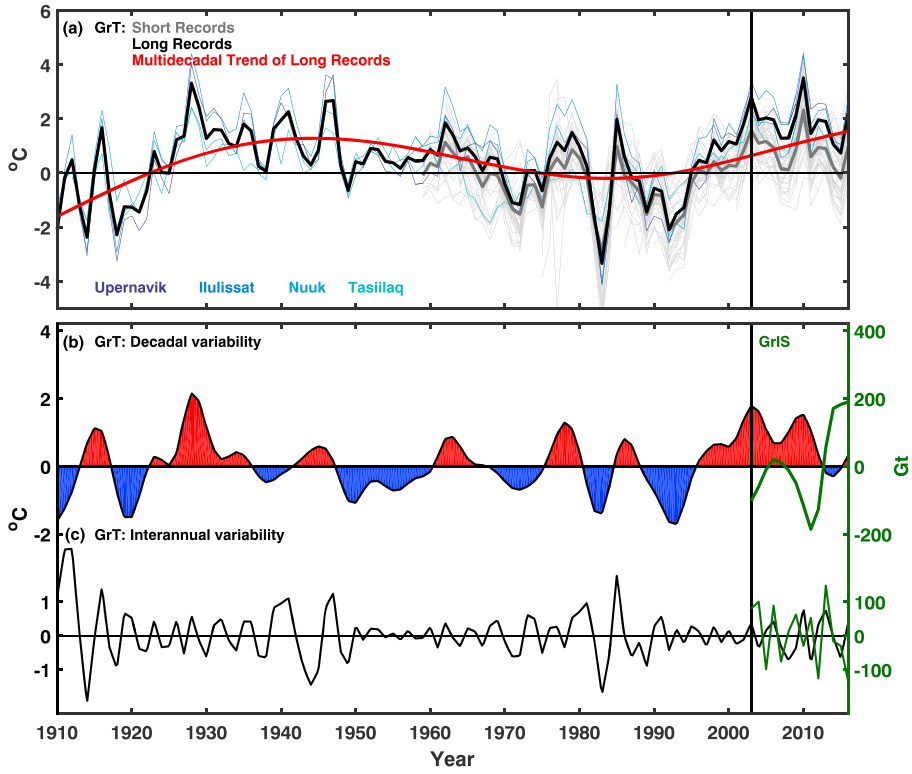


**Figure 8.** Time scales of GrIS mass and GrT. (a) The summer GrT from four stations in Greenland operated by the Danish Meteorological Institute. The black line denotes the mean of four stations with century-long record (color lines). The gray lines show the observations since 1958. The red line is the multidecadal trend derived by EEMD decomposition of the summer GrT (black line). (b) The decadal variability of the summer GrT (black line) and the GrIS (green line) derived by EEMD. (c) The interannual variability of the summer GrT (black line) and the GrIS (green line). GrIS = Greenland Ice Sheet; GrT = Greenland temperature; EEMD = Ensemble Empirical Mode Decomposition.

temperature is nearly 1.6 °C less (Figure 6). The cooling of the ocean is not only helpful for the atmospheric configuration over Greenland but also favorable for the reduction of mass loss due to warmer water intrusion into the marine-terminated glaciers, though the latter process explains only around 30–50 Gt of the total mass budget of the GrIS (Box et al., 2009; Tedstone et al., 2013; Zwally et al., 2002).

From these large-scale spatial patterns in the SLP, Z500, and in the northern North Atlantic Ocean associated with the GrIS mass change, we could deduce that the deceleration of GrIS melt since 2013 may not quickly stop and reverse to previous accelerated state.

### 3.3. Time Scale of the Deceleration of GrIS Mass Loss

It is difficult to deterministically identify whether the deceleration in GrIS melt during 2013–2016 is part of a long-term trend or part of natural variability on short to medium time scales, owing to the absence of a long-term GRACE satellite record. The projection of possible future trends of the GrIS mass based on such short time series record should also proceed very cautiously (Howat & Eddy, 2011). However, the Greenland surface melting suggested by the GRACE satellite record is consistent with the observed surface air temperature variability (Tedesco et al., 2011). There are 72 weather stations in Greenland (Figure 7), of which 68 stations have maintained temperature observations since 1958 and four have century-long continuous records. Although most of these stations are located around the coast, the temperature at these stations varies coherently on decadal and multidecadal time scales (Figure 8a). Using these, we can investigate the time scales of the acceleration in GrIS melt during 2003–2012 and the deceleration since 2013, using the mean summer temperatures of these four stations which have century-long records. This mean temperature is denoted as the observed Greenland mean summer surface temperature, referred to as GrT.

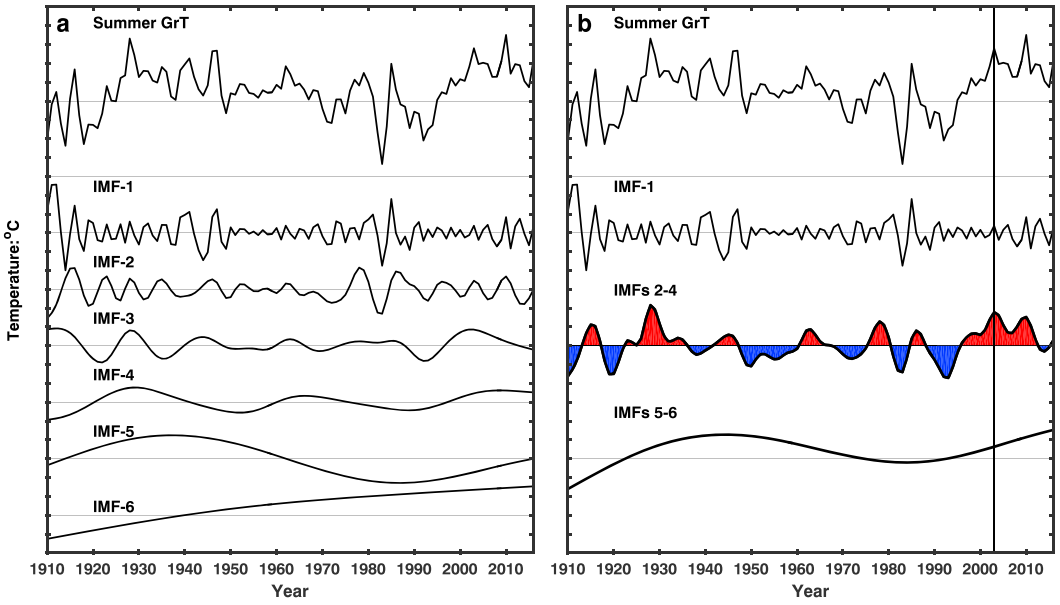


**Figure 9.** Individual IMFs and combined IMFs of GrT. (a) Summer GrT time series and its IMFs (from top to bottom). (b) Combined IMFs2–4 and IMFs5–6, respectively. Vertical solid line in (b) denotes 2003, the starting year of GRACE observations. IMFs = intrinsic mode functions; GrT = Greenland temperature sNAO = summer North Atlantic Oscillation; GrT = Greenland temperature.

We perform EEMD on the GrIS melt and on the summer GrT time series. The GrIS melt time series is decomposed into two nearly orthogonal IMFs. Thus, IMF1, whose mean time scale is around 2.5 years, exhibits neither increasing nor decreasing trends, while IMF2 captures most of the variability of the GrIS melt (Figure 8b). The summer GrT time series can be decomposed into six nearly orthogonal IMFs, whose sum is identical to the summer GrT itself. By means of this construction, the individual IMFs, shown in Figure 9, were found to exhibit preferred mean time scales of 2.7, 8.4, 18.5, 39.8, and 98.2 years, and the last IMF is the long-term warming trend. By computing the correlation coefficients between the IMF2 of the GrIS melt time series and the combinations of the different IMFs of the summer GrT in the period 2003–2016, we found that the highest correlation ($r = -0.71$, $p < 0.001$) is obtained only when IMFs 2, 3, 4 of the summer GrT, which are on decadal and interdecadal time scales, are combined (see section 2.3). The projections of the SLP and Z500 during 1910–2010 upon the combined IMFs 2–4 (Figure 5c) also present a fundamental agreement in structure with Figure 5a, which shows the strong west-east (Greenland-northwest Europe) SLP gradient and the positive correlation between SLP and summer GrIS mass over Greenland and the adjacent North Atlantic subpolar gyre, though rapid Arctic change exerts a different character over the Arctic since the 1980s. This shows that the recent deceleration of the GrIS melt is the result of a combination of the physical decadal and interdecadal variability.

On this decadal time scale, the amplitude of the internal variability of the GrIS melt is around 127.9 Gt. It is nearly half of the general warming trend of the GrIS melting during the GRACE era, around 240.9 Gt, estimated as the difference between the net annual increase and the decrease in the volume of the GrIS (Figures 1b and 1c). This shows that the internal variability of the GrIS mass change driven by the increased total cloud cover during positive sNAO can slow down but cannot stop the trend of the GrIS mass loss under a warming climate. Therefore, we could project that when the sNAO becomes persistently negative, the internal variability of North Atlantic air-sea-ice interactions will inevitably enhance the loss in the volume of the GrIS. Greenland may well therefore experience even faster rates of ice sheet melting than has been observed over the previous two decades, if the secular trend in increasing greenhouse gas emissions continue.

## 4. Discussion

Our finding highlights the importance of internal variability of the GrIS in response to the North Atlantic air-sea interactions, on decadal time scale. The internal variability seems weak when compared to the

trend for long-term loss of the GrIS under the unrelenting anthropogenic warming, but it can mask or enhance the human-induced changes for decades and introduces uncertainties to the estimated projections of the rate of future GrIS melting and global sea level rise.

As shown in Figure 9, the last two IMFs of the summer GrT, representing the multidecadal variability and the secular warming trend of Greenland temperature, respectively, both exhibit monotonic warming trends during the GRACE satellite era. This indicates that GrIS melt during the last two decades is attributable to a combination of both the secular trend of global warming during last century and the multidecadal variability of Atlantic Ocean. During the last century, if the relationship between the summer GrT and the melt of the GrIS has remained unchanged, the multidecadal variability of the summer GrT (Figure 9) implies that the melting of GrIS mass, and hence the GrIS, may have experienced serious retreat (GSML rise) during the 1920–1940s, gradual recovery (GMSL fall) during the 1950–1970s, and dramatic decreasing trends since then (accelerated GMSL rise). Although whole ice sheet mass observations covering Greenland are not available before the GRACE era, snapshots of the terminal locations of many individual land and marine glaciers around Greenland do present observations of the quasiperiodic recessions and advances in the GrIS on the multidecadal time scale (Weidick, 1995), especially the accelerated retreat in response to early twentieth century warming (1920–1950; Weidick, 1968; Box & Herrington, 2007; Williams et al., 2012). The multidecadal oscillation of the GrIS is also indirectly confirmed by the temperature proxy measurements derived from ice cores obtained during Greenland Ice Sheet Project Two (Chylek et al., 2012; Zhou et al., 2016). All of these evidences, especially the records of the recent slowdown in melt, suggest that careful estimation of the internal natural variability of the GrIS is essential for improving our projections of the future ice sheet mass balance and the global sea level change.

## Author contributions

R. R. and X. C. undertook the computation and analysis and led the drafting of this article with contributions from all coauthors. J. Z., W. P., R. M., M. Z., and Y. D. contributed to the calculation of cyclone variability and analysis of cyclone; L. D. processed the Greenland Ice Sheet and temperature analysis. L. W. provided interpretations of atmospheric circulation influence and the surface energy budget. All authors contributed significantly to the drafting of this article.

## Competing interests

The authors declare no competing interests.

**Acknowledgments**
The work is supported by the National Key Basic Research Program of China under grant 2015CB953900, and National Natural Science Foundation of China under grant 41825012 and 41776032). The data sets used in this study are all publicly available; we thank the organizations and providers. They are as follows: (1) GRACE GFZ RL05 level-3 data, the liquid water equivalent thickness from satellite observation during 2002–2017 available in ftp://podaac-ftp.jpl.nasa.gov/allData/tellus/L3/land_mass/RL05/netcdf/; (2) daily surface melt data (National Snow and Ice Data Center) provided by Thomas Mote at University of Georgia since 1979, available at http://nsidc.org/greenland-today/greenland-surface-melt-extent-interactive-chart/; (3) ERA-Interim global reanalysis data, monthly means of daily forecast accumulations surface total precipitation and snowfall since 1979, available at http://www.ecmwf.int/en/research/climate-reanalysis/reanalysis-datasets/era-interim; ERA-20C ECMWF Public Dataset is available at https://www.ecmwf.int/en/forecasts/datasets/archive-datasets/reanalysis-datasets/era-20c; (4) NOAA High Resolution Blended Analysis SST data, daily optimum interpolation sea surface temperature during 1982–2016, which is provided by the NOAA/OAR/ESRL PSD, Boulder, Colorado, USA, from their Web site at https://www.esrl.noaa.gov/psd/; (5) the data sets from Danish Meteorological Institute (DMI) are introduced in DMI Report No. 18-08 (John Cappelen; Weather observations from Greenland 1958–2017) and DMI Report No. 18-04 (John Cappelen (ed.); Greenland—DMI Historical Climate Data Collection 1784–2017). The weather stations in Greenland provide continuous temperature observations. We use 72 weather stations in Greenland, of which 68 started their temperature observations in 1958, and four of them have century-long continuous records. The position of the stations is shown in Figure 7. Data are available at http://www.dmi.dk/laer-om/generelt/dmi-publikationer/2013/; (6) NCEP-NCAR Reanalysis 1 data set for heat flux and cloud variability during 1948–2017, available in http://www.esrl.noaa.gov/psd/data/gridded/data.ncep.reanalysis.derived.html; and (7) the total cloud cover is obtained from CERES, which is available at https://ceres.larc.nasa.gov.

## References

Allan, R. P. (2011). Combining satellite data and models to estimate cloud radiative effect at the surface and in the atmosphere. *Meteorological Applications*, *18*(3), 324–333. https://doi.org/10.1002/met.285

Banzon, V., Smith, T. M., Chin, T. M., Liu, C., & Hankins, W. (2016). A long-term record of blended satellite and in situ sea-surface temperature for climate monitoring, modeling and environmental studies. *Earth System Science Data*, *8*(1), 165–176. https://doi.org/10.5194/essd-8-165-2016

Belleflamme, A., Fettweis, X., & Erpicum, M. (2015). Recent summer Arctic atmospheric circulation anomalies in a historical perspective. *The Cryosphere*, *9*(1), 53–64. https://doi.org/10.5194/tc-9-53-2015

Bevis, M., Harig, C., Khan, S. A., Brown, A., Simons, F. J., Willis, M., et al. (2019). Accelerating changes in ice mass within Greenland, and the ice sheet's sensitivity to atmospheric forcing. *PNAS*, *116*(6), 1934–1939. https://doi.org/10.1073/pnas.1806562116

Box, J. E., Fettweis, X., Stroeve, J. C., Tedesco, M., Hall, D. K., & Steffen, K. (2012). Greenland Ice Sheet albedo feedback: Thermodynamics and atmospheric drivers. *The Cryosphere*, *6*(4), 821–839. https://doi.org/10.5194/tc-6-821-2012

Box, J. E., and A. Herrington (2007), Was there a 1930's meltdown of Greenland glaciers? [Abstract C11A-0077.] Eos, 88(52), Fall Meet. Suppl.

Box, J. E., Yang, L., Bromwich, D. H., & Bai, L. S. (2009). Greenland Ice Sheet surface air temperature variability: 1840-2007. *Journal of Climate*, *22*(14), 4029–4049. https://doi.org/10.1175/2009JCLI2816.1

Cazenave, A. (2018). Global sea-level budget 1993–present. *Earth System Science Data*, *10*, 1551–1590.

Chen, J. L. (2006). Satellite gravity measurements confirm accelerated melting of Greenland Ice Sheet. *Science*, *313*(5795), 1958–1960. https://doi.org/10.1126/science.1129007

Chen, L. L., Fettweis, X., Knudsen, E. M., & Johannessen, O. M. (2015). Impact of cyclonic and anticyclonic activity on Greenland Ice Sheet surface mass balance variation during 1980–2013. *International Journal of Climatology*, *36*, 3423–3433.

Chen, X., Zhang, X., Church, J. A., Watson, C. S., King, M. A., Monselesan, D., et al. (2017). The increasing rate of global mean sea-level rise during 1993–2014. *Nature Climate Change*, *7*(7), 492–495. https://doi.org/10.1038/nclimate3325

Chen, X. Y., & Tung, K.-K. (2018). Global surface warming enhanced by weak Atlantic overturning circulation. *Nature*, *559*(7714), 387–391. https://doi.org/10.1038/s41586-018-0320-y

Chylek, P., Folland, C., Frankcombe, L., Dijkstra, H., Lesins, G., & Dubey, M. (2012). Greenland ice core evidence for spatial and temporal variability of the Atlantic Multidecadal Oscillation. *Geophysical Research Letters*, *39*, L09705. https://doi.org/10.1029/2012GL051241

Dee, D. P., Uppala, S. M., Simmons, A. J., Berrisford, P., Poli, P., Kobayashi, S., et al. (2011). The ERA-Interim reanalysis: Configuration and performance of the data assimilation system. *Quarterly Journal of the Royal Meteorological Society*, *137*(656), 553–597. https://doi.org/10.1002/qj.828

Enderlin, E. M., Howat, I. M., Jeong, S., Noh, M. J., van Angelen, J. H., & van den Broeke, M. R. (2014). An improved mass budget for the Greenland Ice Sheet. *Geophysical Research Letters*, *41*, 866–872. https://doi.org/10.1002/2013GL059010

Fettweis, X., Hanna, E., Lang, C., Belleflamme, A., Erpicum, M., & Gallée, H. (2013). Important role of the mid-tropospheric atmospheric circulation in the recent surface melt increase over the Greenland Ice Sheet. *The Cryosphere*, *7*(1), 241–248. https://doi.org/10.5194/tc-7-241-2013

Fettweis, X., Mabille, G., Erpicum, M., Nicolay, S., & den Broeke, M. V. (2011). The 1958–2009 Greenland Ice Sheet surface melt and the mid-tropospheric atmospheric circulation. *Climate Dynamics*, *36*(1-2), 139–159. https://doi.org/10.1007/s00382-010-0772-8

Folland, C. K., Knight, J., Linderholm, H. W., Fereday, D., Ineson, S., & Hurrell, J. W. (2009). The summer North Atlantic Oscillation: Past, present, and future. *Journal of Climate*, *22*(5), 1082–1103. https://doi.org/10.1175/2008JCLI2459.1

Franco, B., Fettweis, X., & Erpicum, M. (2013). M. Future projections of the Greenland Ice Sheet energy balance driving the surface melt. *The Cryosphere*, *7*(1), 1–18. https://doi.org/10.5194/tc-7-1-2013

Gregory, J. M., Huybrechts, P., & Raper, S. C. B. (2004). Climatology: Threatened loss of the Greenland ice-sheet. *Nature*, *428*(6983), 616–616. https://doi.org/10.1038/428616a

Hanna, E., Huybrechts, P., Steffen, K., Cappelen, J., Huff, R., Shuman, C., et al. (2008). Increased runoff from melt from the Greenland Ice Sheet: A response to global warming. *Journal of Climate*, *21*(2), 331–341. https://doi.org/10.1175/2007JCLI1964.1

Hanna, E., Huybrechts, P., Steffen, K., Cappelen, J., Huff, R., Shuman, C., et al. (2010). Increased runoff from melt from the Greenland Ice Sheet: A response to global 1. *Journal of Climate*, *21*(2), 331–341. https://doi.org/10.1175/2007jcli1964.1

Hofer, S., Tedstone, A. J., Fettweis, X., & Bamber, J. L. (2017). Decreasing cloud cover drives the recent mass loss on the Greenland Ice Sheet. *Science Advances*, *3*(6), e1700584. https://doi.org/10.1126/sciadv.1700584

Howat, I. M., & Eddy, A. (2011). Multi-decadal retreat of Greenland's marine-terminating glaciers. *Journal of Glaciology*, *57*(203), 389–396. https://doi.org/10.3189/002214311796905631

Hu, A., Meehl, G. A., Han, W., & Yin, J. (2011). Effect of the potential melting of the Greenland Ice Sheet on the Meridional Overturning Circulation and global climate in the future. *Deep Sea Research Part II Topical Studies in Oceanography*, *58*(17-18), 1914–1926. https://doi.org/10.1016/j.dsr2.2010.10.069

Huang, N. E., Shen, Z., Long, S. R., Wu, M. C., Shih, H. H., Zheng, Q., et al. (1998). The empirical mode decomposition and the Hilbert spectrum for nonlinear and non-stationary time series analysis. *Proceedings of the Royal Society of London. Series A: Mathematical, Physical and Engineering Sciences*, *454*(1971), 903–995. https://doi.org/10.1098/rspa.1998.0193

Kalnay, E., Kanamitsu, M., Kistler, R., Collins, W., Deaven, D., Gandin, L., et al. (1996). The NCEP/NCAR 40-year reanalysis project. *Bulletin of the American Meteorological Society*, *77*(3), 437–471. https://doi.org/10.1175/1520-0477(1996)077<0437:TNYRP>2.0.CO;2

Miller, N. B., Shupe, M. D., Cox, C. J., Noone, D., Persson, P. O. G., & Steffen, K. (2017). Surface energy budget responses to radiative forcing at summit Greenland. *The Cryosphere*, *11*(1), 497–516. https://doi.org/10.5194/tc-11-497-2017

Nghiem, S. V., Hall, D. K., Mote, T. L., Tedesco, M., Albert, M. R., Keegan, K., et al. (2012). The extreme melt across the Greenland Ice Sheet in 2012. *Geophysical Research Letters*, *39*, L20502. https://doi.org/10.1029/2012GL053611

Smith, L. C., Chu, V. W., Yang, K., Gleason, C. J., Pitcher, L. H., Rennermalm, A. K., et al. (2014). Efficient meltwater drainage through supraglacial streams and rivers on the south west Greenland Ice Sheet. *Proceedings of the National Academy of Sciences*, *112*(4), 1001–1006. https://doi.org/10.1073/pnas.1413024112

Straneo, F., Hamilton, G. S., Sutherland, D. A., Stearns, L. A., Davidson, F., Hammill, M. O., et al. (2010). Rapid circulation of warm subtropical waters in a major glacial fjord in East Greenland. *Nature Geoscience*, *3*(3), 182–186. https://doi.org/10.1038/ngeo764

Tedesco, M., Fettweis, X., Mote, T., Wahr, J., Alexander, P., Box, J. E., & Wouters, B. (2013). Evidence and analysis of 2012 Greenland records from spaceborne observations, a regional climate model and reanalysis data. *The Cryosphere*, *7*(2), 615–630. https://doi.org/10.5194/tc-7-615-2013

Tedesco, M., Fettweis, X., van den Broeke, M. R., van de Wal, R. S. W., Smeets, C. J. P. P., van de Berg, W. J., et al. (2011). The role of albedo and accumulation in the 2010 melting record in Greenland. *Environmental Research Letters*, *6*(1). https://doi.org/10.1088/1748-9326/6/1/014005

Tedstone, A. J., Nienow, P. W., Sole, A. J., Mair, D. W. F., Cowton, T. R., Bartholomew, I. D., & King, M. A. (2013). Greenland Ice Sheet motion insensitive to exceptional meltwater forcing. *Proceedings of the National Academy of Sciences of the United States of America*, *110*(49), 19719–19724. https://doi.org/10.1073/pnas.1315843110

van Angelen, J. H., Lenaerts, J. T. M., Lhermitte, S., Fettweis, X., Kuipers Munneke, P., van den Broeke, M. R., et al. (2012). Sensitivity of Greenland Ice Sheet surface mass balance to surface albedo parameterization: A study with a regional climate model. *The Cryosphere*, *6*(5), 1175–1186. https://doi.org/10.5194/tc-6-1175-2012

van den Broeke, M., Bamber, J., Ettema, J., Rignot, E., Schrama, E., van de Berg, W. J., et al. (2009). Partitioning recent Greenland mass loss. *Science*, *326*(5955), 984–986. https://doi.org/10.1126/science.1178176

van Tricht, K., Lhermitte, S., Lenaerts, J. T. M., Gorodetskaya, I. V., L'Ecuyer, T. S., Noël, B., et al. (2016). Clouds enhance Greenland Ice Sheet meltwater runoff. *Nature Communications*, *7*(1). https://doi.org/10.1038/ncomms10266

Velicogna, I., & Wahr, J. (2006). Acceleration of Greenland ice mass loss in spring 2004. *NATURE*, *443*(7109), 329–331. https://doi.org/10.1038/nature05168

Walsh, J. E., & Chapman, W. L. (1998). Arctic cloud radiation temperature associations in observational data and atmospheric reanalyses. *Journal of Climate*, *11*(11), 3030–3045. https://doi.org/10.1175/1520-0442(1998)011,3030:ACRTAI.2.0.CO;2

Weidick, A. (1968), Observations on some Holocene glacier fluctuations in west Greenland. Meddelelser om Grønland 165, 202 pp.

Weidick, A. (1995), Satellite image atlas of glaciers of the world, Greenland (USGS Professional Paper 1386-C, United States Government Printing Office, Washington)

Williams, R. S. Jr., & Ferrigno, J. G. (Eds.) (2012). *State of the Earth's cryosphere at the beginning of the 21st century: Glaciers, global snow cover, floating ice, and permafrost and periglacial environments. U.S. Geological Survey Professional Paper 1386–A* (p. 546).

Wu, Z., & Huang, N. E. (2009). Ensemble empirical mode decomposition: A noise-assisted data analysis method. *Advances in Adaptive Data Analysis*, *01*(01), 1–41. https://doi.org/10.1142/S1793536909000047

Zhou, J., Tung, K. K., & Li, K. F. (2016). Multidecadal variability in the Greenland ice core records obtained using intrinsic timescale decomposition. *Climate Dynamics*, *47*(3-4), 739–752. https://doi.org/10.1007/s00382-015-2866-9

Zwally, H. J., Abdalati, W., Herring, T., Larson, K., Saba, J., & Steffen, K. (2002). Surface melt-induced acceleration of Greenland Ice-Sheet flow. *Science*, *297*(5579), 218–222. https://doi.org/10.1126/science.1072708